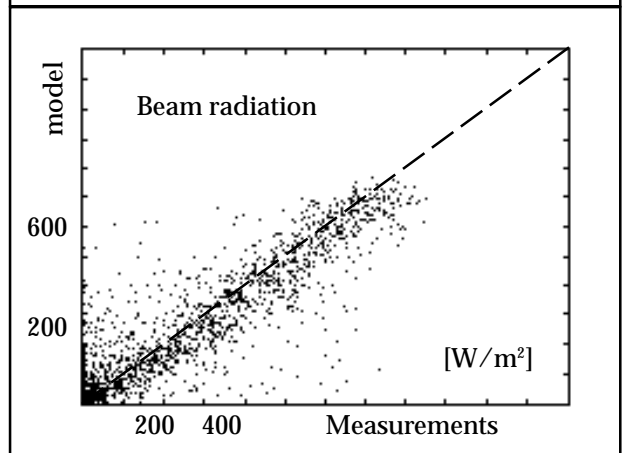
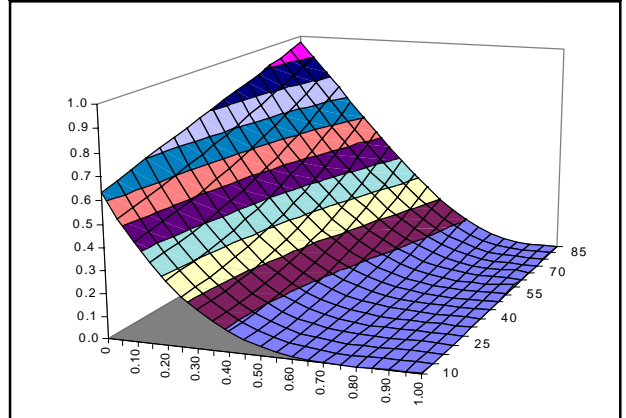
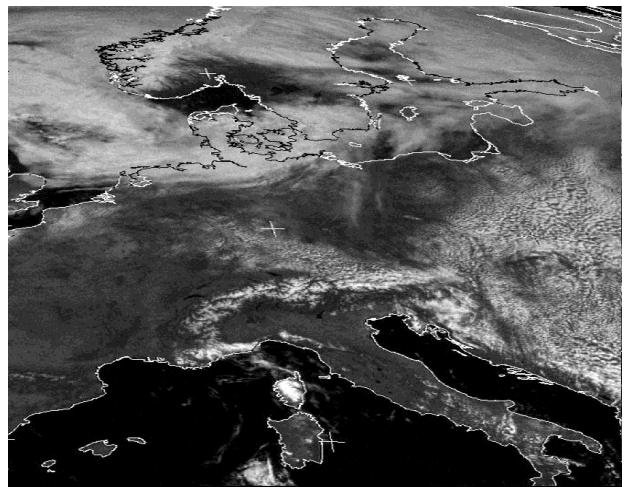


Satellite

Commission of the European Communities

# Radiation and illuminance components from meteosat images



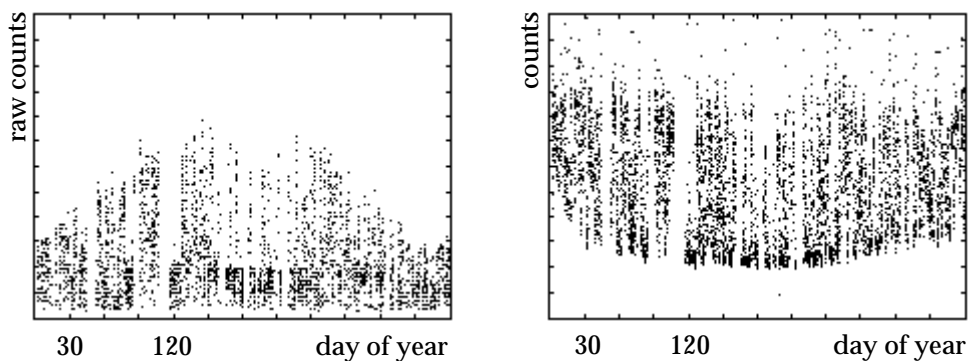
Working paper, Pierre Ineichen  
GAP-E, University of Geneva  
4th satellight meeting  
Oldenburg, June 4-5, 1997

## Introduction

During the derivation of our models, we had difficulties at low solar elevations and at low sun-satellite angles, due to the lack of data and/or the zero ground reflectance values. We decided to return to the raw counts and to do geometric corrections on the counts before to derive the cloud index.

## Raw satellite counts

The raw counts from the Meteosat satellite have to be corrected for different geometrical effects: the earth-sun distance variation, the sun elevation, the backscatter light, the air-mass effect, etc. These counts have the following aspect when plotted against day of the year, without any correction (left figure):

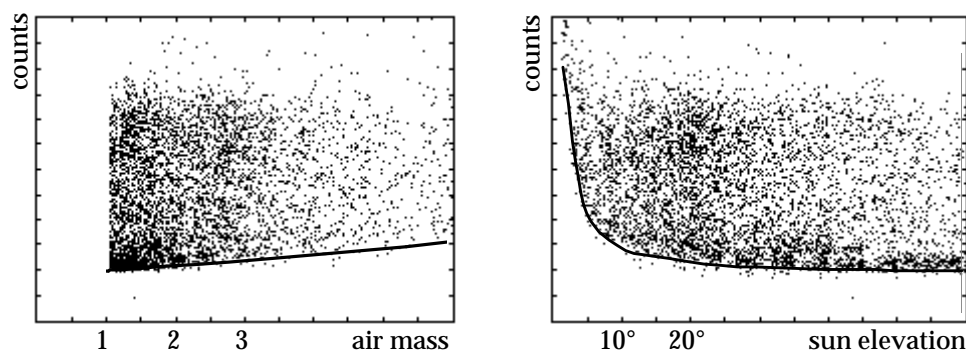


Raw counts for the pixel over the station of Geneva, for the period of April 1st 1994 to March 31, 1995. On the second figure, the sun-earth distance and the sun elevation corrections were applied.

On the second graph, two effects can be emphasized: the seasonal and the snow effect. Due to the geometry and/or the ground reflection coefficient, the counts are lower in summer than in winter, and there is an important effect in the first 15 day of January, where there was snow on the ground over the region of Geneva.

## Air mass effect

The air mass effect is the most important and occurs at low sun elevation. During its way through the atmosphere, the sun ray is diffused and scattered by the atmosphere components and a part of this diffusion is measured by the satellite. The following figures represent the satellite counts versus the air mass and the sun elevation:

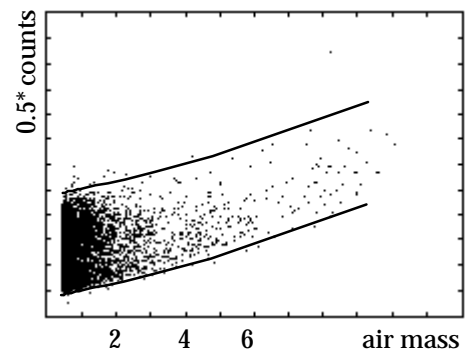


Counts versus air mass (left) and versus sun elevation. The lines represent the estimation of the lower boundary and will be applied on the counts as air-mass effect correction to normalize the counts.

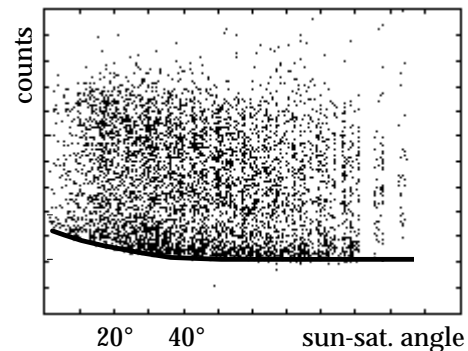
This effect, for a cloudless sky can be estimated as exponentially proportional to the crossed air mass. Even if the effect is not the same for cloudless skies and overcast skies, in a first approximation, one can apply the same correction for all conditions. This can be seen on the next graph where the scales were contracted. A more important data bank is necessary to improve this correction. Even if it can be estimated theoretically, the coefficients have to be adapted to the data.

### Backscatter effect

It is well known that there is a backscatter effect when the sun and the satellite are in the same axis (the sun is behind the satellite). This effect can be shown on a graph representing the counts versus the sun-satellite angle. It has to be noticed that this effect is independent of the previous: the air-mass effect is important at low solar elevation and the backscatter effect is visible up to 30°-40° of sun-satellite angle, conditions with high sun elevations. The next graph shows this effect. The formulation of the correction is represented by a line on the graph.



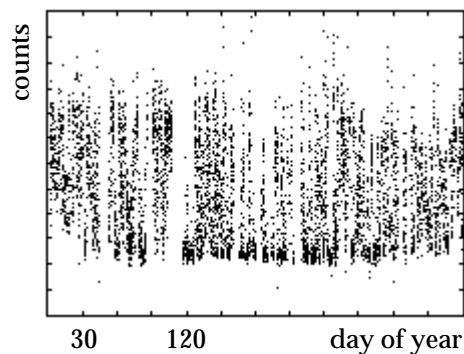
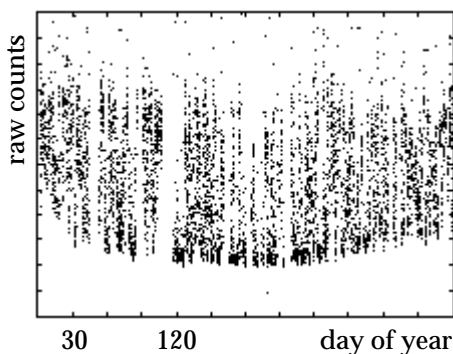
Counts versus air mass. As a first estimation, the same correction will be applied on all sky conditions.



Counts versus sun-satellite angle. The backscatter effect is clear up to 30°. The line is the correction that will be applied on the counts

### Cloud index

When these corrections are applied, one obtains the following figure (on the right) for the counts versus the day of the year. Except for the first period of January where there was snow in the region of Geneva, it is now possible to determine a lower boundary for the counts. On the basis of the figure and in a first approximation, we will take a constant value over the year. For the upper limit, the raw air-mass correction can be improved with more input data, but an upper limit can also be determined on the graph. A linear distribution between these two lines will give the cloud index.

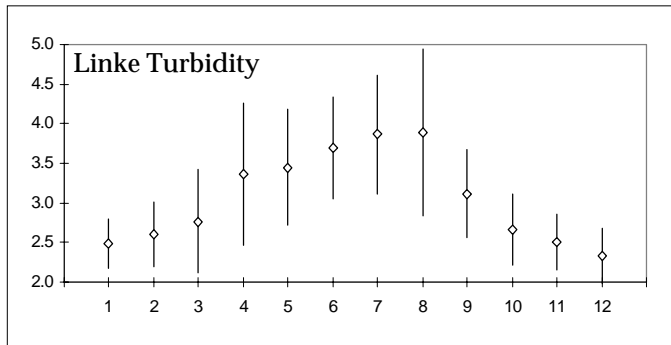


On the left graph, the sun-earth distance and the sun elevation correction were applied. The counts on the right graph take into account the air mass and the backscatter effects and will be used to derive the cloud index.

### Clear sky model

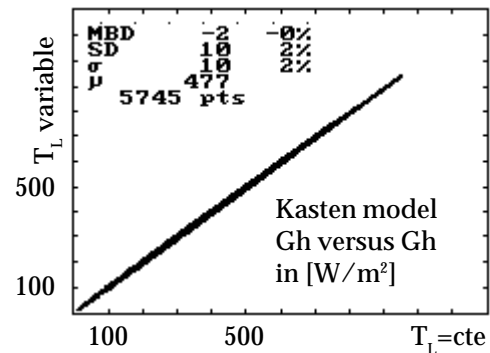
There are a lot of clear sky models available, taking into account the turbidity or not. We tested some of them with the data of Geneva. If a constant value of 3 is taken for the Linke

turbidity, all the good models give slightly the same results. On the basis of precise data taken in Geneva between 1991 and 1997, the following values for the turbidity were obtained on a monthly basis:



Average monthly Linke turbidity coefficients for the station of Geneva over a period from 1991 to 1997

In this study, we used the Kasten turbidity dependant clear sky model. This model was tested over 80 Anetz stations of the Swiss Meteorological network and gives very good results, even for high altitude stations. When comparing the model with a constant value of Linke turbidity ( $T_L = 3$  for Geneva) and the above values, the mean bias difference is 2 [W/m<sup>2</sup>] and the root mean square difference is 10 [W/m<sup>2</sup>] (mean global : 477 [W/m<sup>2</sup>]). This effect is very low compared to the dispersion obtained with the radiation derivation models.



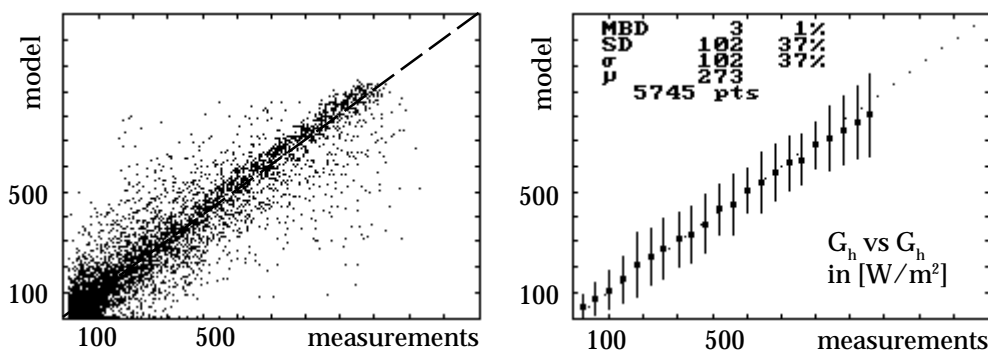
Kasten clear sky model for the evaluation of the global horizontal radiation. Comparison between variable and constant Linke Turbidity

### Global derivation

Using the cloud index and the Kasten clear sky model, the global can be derived by

$$G_h = G_{hc} * (1 - n)$$

This formulation is very simple but gives zero values for the global radiation when the cloud index is equal to the unity. Using this very simple «model», we obtained with Geneva's data the following results:



Evaluation of the global horizontal radiation on one year data from Geneva. The ground reflexion is taken constant and no correction is made for the snow in January.

To avoid zero values for the global radiation, we made a regression between cloud index and normalized global radiation. Representing these two quantities for different sun eleva-

tions, one can point out a slightly varying correlation with the sun elevation. To visualize this variation and to do a curve fitting, we reduced the data into cloud index bins for 6 sun elevations (see appendix). We then made a two variables regression on the reduced data and obtained a negligible mean bias difference (MBD) between model and measurements, and a root mean square difference (RMSD) reduced to 34% (94 W/m<sup>2</sup>). The station of Geneva is not situated in the middle of a geographic pixel, and the radiation parameters are integrated over the 10 minutes around the meteosat measurements time ( $\pm 5$  min.); it is therefore difficult to be sure that the radiation corresponds to the pixel value. To evaluate the real precision of the model, we reduced the data bank to stable conditions: the variation from one pixel to the other in the 3x3 pixels around Geneva has to be within  $\pm 5\%$ . In these conditions, the MBD becomes -2% and the RMSD is equal to 29% (78 W/m<sup>2</sup>).

### Other radiation and illuminance components derivation

We followed exactly the same approach for all the other radiation and illuminance components, and obtained the following results (the luminance was derived from the v2n model):

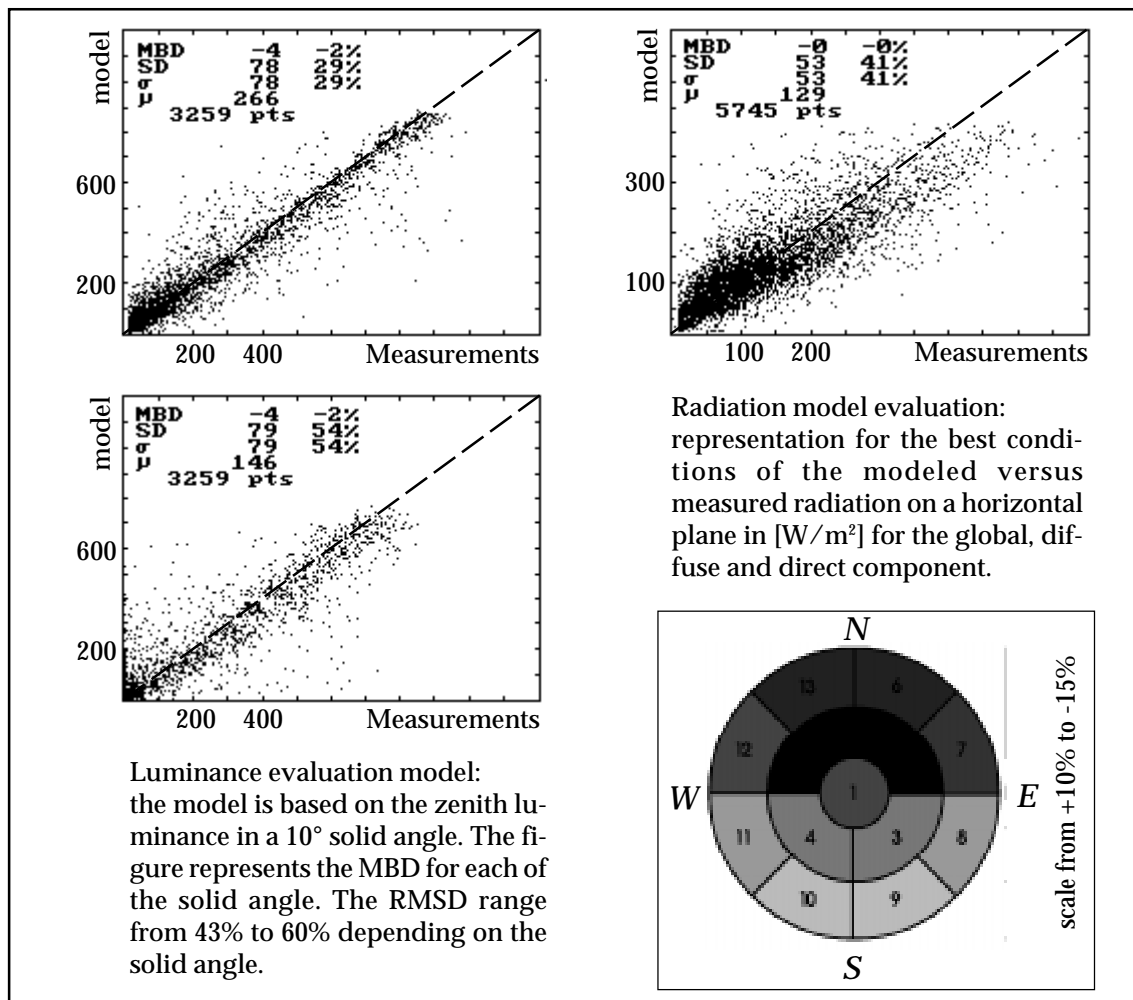
Irradiance	mean	MBD		SD		RMSD	
	[W/m2]	[W/m2]	[%]	[W/m2]	[%]	[W/m2]	[%]
Global - v2n	301	38	13%	107	36%	113	38%
Global	273	-4	-1%	93	34%	93	34%
Diffuse	129	0	0%	53	41%	53	41%
Beam	143	-6	-4%	97	68%	97	68%
Gh-Dh	143	-3	-2%	94	66%	94	66%
Homogeneous							
Global	266	-4	-2%	78	29%	78	29%
Diffuse	120	-1	-1%	51	43%	51	43%
Beam	147	-7	-5%	82	56%	82	56%
Gh-Dh	147	-4	-3%	79	54%	79	54%
Illuminance	[hlux]	[hlux]	[%]	[hlux]	[%]	[hlux]	[%]
Global	269	3	1%	89	33%	89	33%
Diffuse	148	1	1%	56	38%	56	38%
Beam	111	-10	-9%	83	75%	84	76%
Beam	111	12	11%	85	77%	86	77%
Luminance	[cd]	[cd]	[%]	[cd]	[%]	[cd]	[%]
zenith	4347	158	4%	2271	52%	2276	52%
scan	5332	-288	-5%	3107	58%	3120	59%
north	3393	-696	-21%	1809	53%	1939	57%
e/w	2810	-75	-3%	2150	77%	2151	77%
south	7196	113	2%	4054	56%	4056	56%

From this table, the following conclusions can be drawn:

- the v2n global is in this table only for comparison purpose. The cloud index values issued by the v2n model are biased by the ground albedo equal to zero for all data with sun elevation lower than 10° and very high in April (twice the average annual value),
- the determination of the diffuse and the global components gives very good results if one keep in mind that the only input parameter is a reflectance,

- the homogeneous cases give very good results for the global derivation. The comparison with the RMSD obtained with all the data shows that it is not «a priori» the geographic pixel that is the right pixel: if strong meteorological wind is blowing, the next pixel in the wind direction will give better results.
- the global-diffuse difference gives slightly better results than the direct model. This can be explained by a lot of zero beam values influencing the regression and could be improved with a better determination of the bins for the derivation of the model.
- the luminance evaluation is based on the v2n cloud index and therefore has to be done with the new cloud index. For all the components the dispersion was improved with new cloud index and it can be assumed that it will also be the case with the luminance determination.
- these models are fitted and evaluated on the same data bank. It is clear that they have to be assessed on more data for other geographic and climatic sites.

Below is a graphic summary of the results we obtained on the Geneva's data and our models:

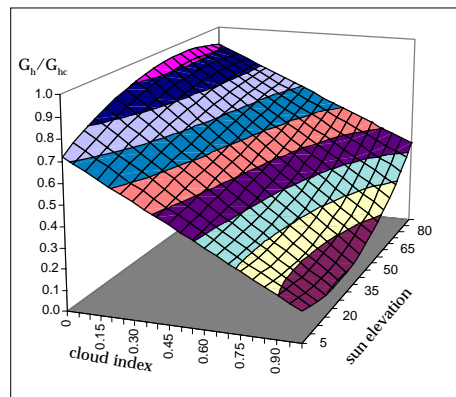
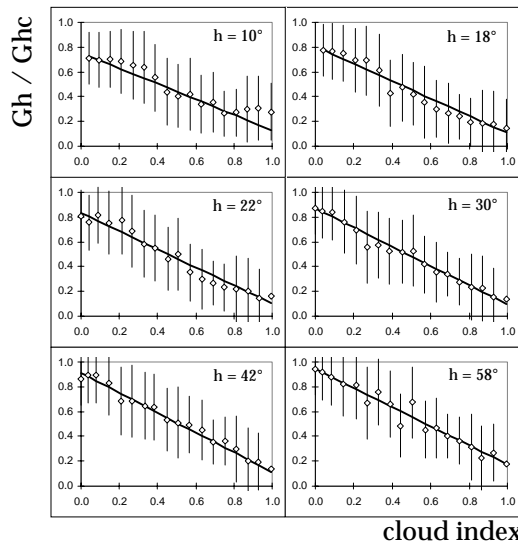


## Conclusion

The above results show that the direct way from pixel to radiation and illuminance components gives good results. The models have to be derived and assessed on a wide geographic and climatic range.

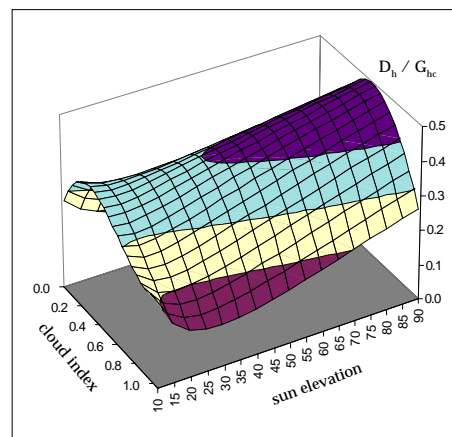
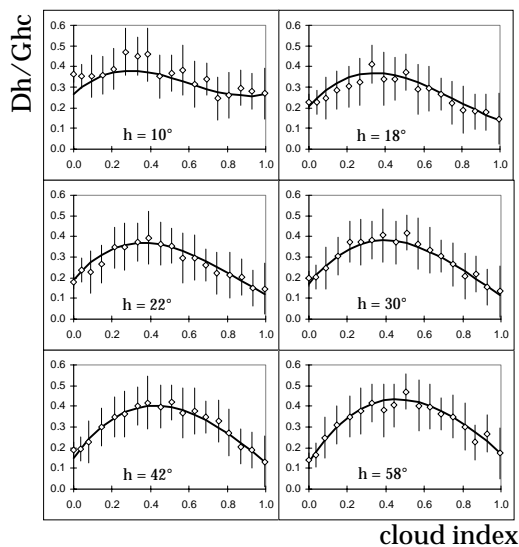
# Appendix

Global radiation:



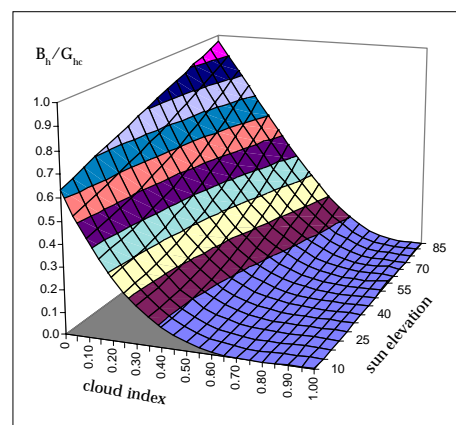
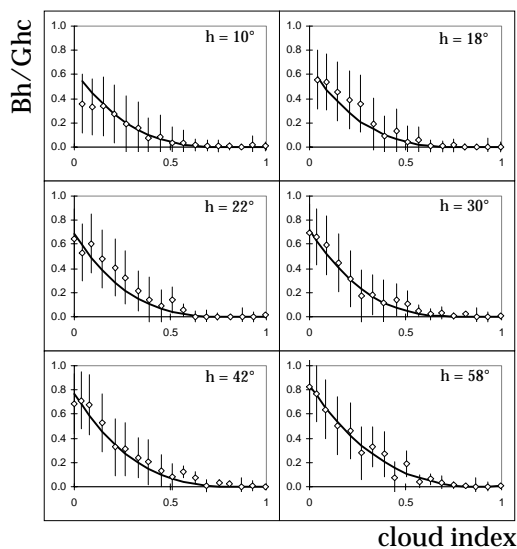
Derivation of the global correlation with the cloud index and the sun elevation

Diffuse radiation:



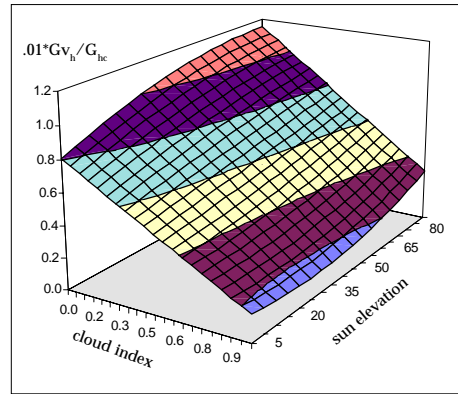
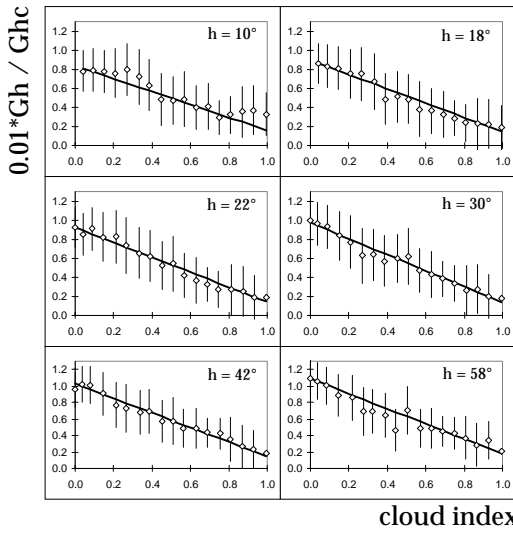
Derivation of the diffus correlation with the cloud index and the sun elevation

Beam radiation:



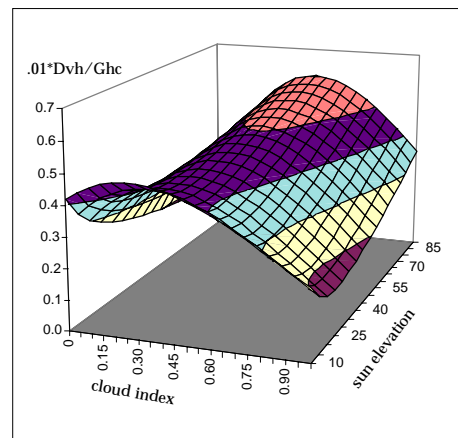
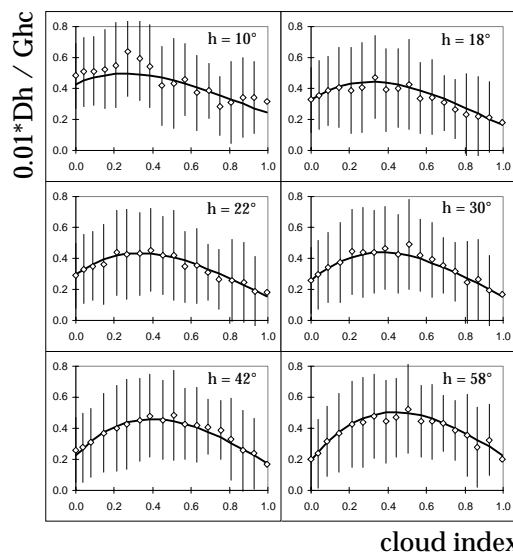
Derivation of the beam correlation with the cloud index and the sun elevation

Global illuminance:



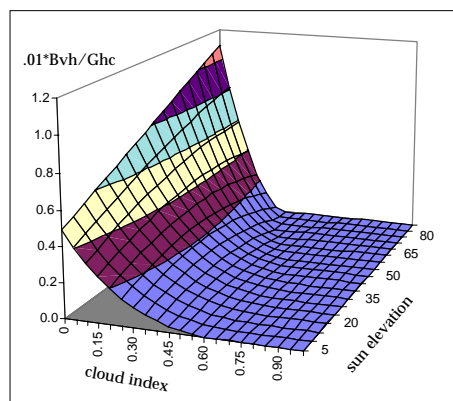
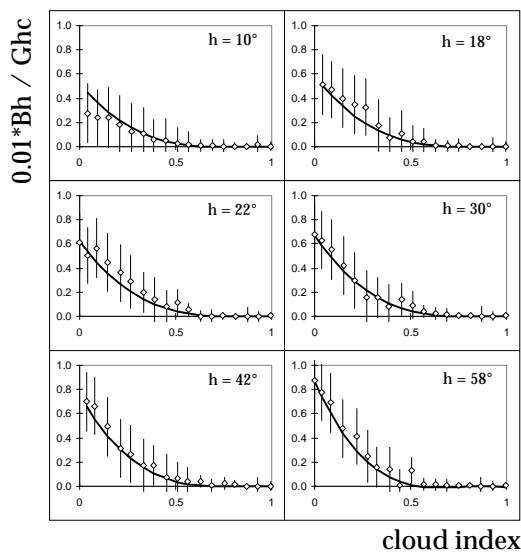
Derivation of the global correlation with the cloud index and the sun elevation

Diffuse illuminance:



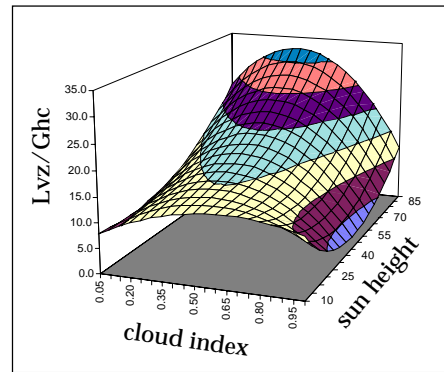
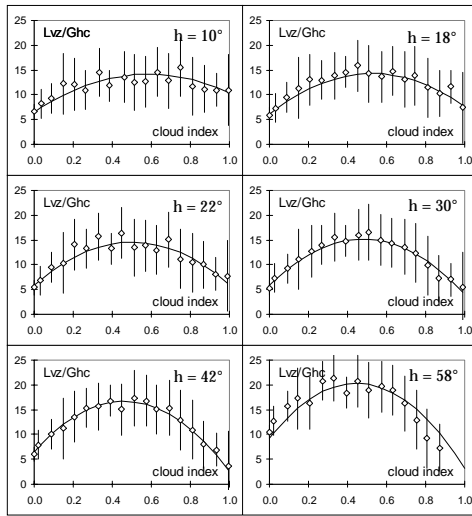
Derivation of the diffuse correlation with the cloud index and sun elevation

Beam illuminance:



Derivation of the beam correlation with the cloud index and the sun elevation

Zenith luminance:



Derivation of the zenith luminance correlation with the cloud index and the sun elevation